

PLENARY SESSION

DARK MATTER AND DARK ENERGY IN THE COMA CLUSTER OF GALAXIES

G.S. Bisnovatyi-Kogan^{1,2}, A.D. Chernin³

¹Space Research Institute RAS., Moscow, Russia, *gkogan@rssi.ru*

²National Research Nuclear University MEPhI, Moscow, Russia,

³Sternberg Astronomical Institute, MSU, Moscow, Russia, *artur.chernin@gmail.com*

ABSTRACT. The Coma cluster of galaxies is studied as a giant aggregation of dark matter and baryons embedded in the dark energy background. Key theory relations for the local dark-energy effects are given. On the basis of the theory and current observational data, three characteristic masses of the Coma cluster are introduced and evaluated. A new dark matter mass profile is suggested and used to find the upper bounds on the total mass and total size of the cluster. A solution is obtained for the hydrodynamic outflow of the polytropic gas from the gravitating center, in presence of the uniform Dark Energy (DE). The main property of the wind in presence of DE is its unlimited acceleration after passing the critical point. In application of this solution to the winds from galaxy clusters we suggest that collision of the strongly accelerated wind with another galaxy cluster, or with another galactic cluster wind could lead to the formation of a highest energy cosmic rays.

Key words: galaxies: the Coma Cluster, dark matter, dark energy, gas outflow

1. Introduction

We study the famous Coma cluster of galaxies where dark matter was originally found by Zwicky (1933,1937). Zwicky used the virial theorem to show that non-luminous dark matter dominated the cluster on megaparsec scales. He estimated the cluster total mass as $3 \times 10^{14} M_{\odot}$, if to normalize his figure to the presently adopted value of the Hubble constant $h = 0.71$ which is used hereafter. A half-century later, The & White (1986) found an order of magnitude larger value, $2 \times 10^{15} M_{\odot}$, with a modified version of the virial theorem. Hughes (1989, 1998) obtained a similar value $(1 - 2) \times 10^{15} M_{\odot}$ with X-ray data under the assumption that the cluster hot intergalactic gas is in hydrostatic equilibrium. With a similar assumption, Colles (2006) reports the mass $4.4 \times 10^{14} M_{\odot}$ inside the radius of 1.4 Mpc. A weak-lensing analysis gave the mass of $2.6 \times 10^{15} M_{\odot}$ (Kubo et al. 2007) within 4.8

Mpc radius. Geller et al. (1999, 2011) extended mass estimates to the outskirts of the cluster using the caustic technique (Diaferio & Geller 1997, Diaferio 1999) and found the mass $2.4 \times 10^{15} M_{\odot}$ within the 14 Mpc radius. Taken the figures at face value, one may see that the mass within 14 Mpc appears to be smaller than the mass within 4.8 Mpc. Most probably, this is due to uncertainties in mass determination. Indeed, the 2σ error is $1.2 \times 10^{15} M_{\odot}$ in Geller's et al. (1999,2011) data, and within this uncertainty, the result does not contradict the small-radius data.

In this paper, we consider the Coma cluster as a giant gravitationally bound aggregation of dark matter and baryons embedded in the uniform background of dark energy. Is antigravity produced by dark energy significant in the volume of the cluster? Does it alternate the structure of the cluster? Can antigravity put limits on the major gross parameters of the system? Addressing these questions, we continue our efforts to clarify and quantify the local gravity-antigravity interplay on the spatial scales of $\sim 1 - 10$ Mpc (Chernin 2001,2008,2013, Bisnovatyi-Kogan and Chernin 2012).

A solution is presented of hydrodynamic equations for the winds from galactic clusters in presence of DE. It is a generalized solution for the outflows from the gravitating body, obtained for solar and stellar winds by Stanyukovich (1955) and Parker (1963), to the presence of DE. It implies significant changes in the structure of solutions describing galactic winds, what had been investigated in the paper of Bisnovatyi-Kogan and Merafina (2013).

2. Local antigravity produced by dark energy

The local dynamical effects of dark energy can adequately be described in terms of Newtonian mechanics, if the force field it produces is weak in the standard sense. Such an approach borrows from General Relativity the major result: the effective gravitating density of a uniform medium is given by the sum

$$\rho_{\text{eff}} = \rho + 3P, \quad (1)$$

where ρ and P is the density and pressure of a uniform fluid (the speed of light is 1 hereafter). The dark energy equation of state is $P_{DE} = -\rho_{DE}$, and its effective gravitating density is negative:

$$\rho_{DEeff} = \rho_{DE} + 3P_{DE} = -2\rho_{DE} < 0, \quad (2)$$

which means that dark energy produces antigravity.

Einstein's "law of universal antigravity" says that two bodies imbedded in the dark energy background are repulsed from each other with a force that is proportional to the distance r between them:

$$F_E(r) = -\frac{4\pi G}{3}\rho_{DEeff}r^3/r^2 = +\frac{8\pi G}{3}\rho_{DE}r. \quad (3)$$

Eq.(3) may be use to describe the force field produced by a spherical matter mass M_M and the uniform dark energy background in which the mass is embedded:

$$F(R) = F_N(R) + F_E(R) = -G\frac{M_M}{R^2} + \frac{8\pi G}{3}\rho_{DE}R. \quad (4)$$

Eq.4 shows that the net force $F(R)$ is zero at the distance

$$R = R_{ZG} = \left[\frac{M_M}{\frac{8\pi}{3}\rho_{DE}}\right]^{1/3} = 11\frac{M_M}{10^{15}M_\odot} \text{ Mpc}. \quad (5)$$

Here the observed value of the dark energy density $\rho_{DE} = 0.7 \times 10^{-29} \text{ g/cm}^3$ is used. The critical physical parameter R_{ZG} is the zero-gravity radius (Chernin 2001). Gravity dominates at distances $R < R_{ZG}$, while antigravity is stronger than gravity at $R > R_{ZG}$.

3. Three masses of the cluster

The presence of dark energy in the volume of a cluster like the Coma cluster may be quantified by the effective gravitating mass of dark energy within a given clustrocentric radius R :

$$M_{DE}(R) = \frac{4\pi}{3}\rho_{DEeff}R^3 = -\frac{8\pi}{3}\rho_{DE}R^3 \quad (6)$$

$$-0.85 \times 10^{12} \left[\frac{R}{1 \text{ Mpc}}\right]^3 M_\odot.$$

The matter (dark matter and baryons) content of the cluster is characterized (in the spherical approximation) by the mass $M_M(R)$ inside the radius R :

$$M_M(R) = 4\pi \int \rho(R)R^2 dR. \quad (7)$$

Here $\rho(R)$ is the matter density within the sphere of the radius R inside the cluster. The sum

$$M_G(R) = M_M(R) + M_{DE}(R), \quad (8)$$

is the total gravitating mass within the radius R . Since dark matter and dark energy reveal themselves in observations via their gravitation only, it is the mass $M_G(R)$ that is only available for astronomical measurements. Identifying $M_G(R)$ with the value $2.4 \times 10^{15} M_\odot$ found in the Coma observations (Geller et al.1999) for the radius $R = 14 \text{ Mpc}$, we find for this radius:

$$M_{DE} = -2.3 \times 10^{15} M_\odot, \quad M_M = 4.7 \times 10^{15} M_\odot \simeq 2M_G. \quad (9)$$

As we see, the absolute value of the dark energy mass M_{DE} is (almost exactly) equal to the gravitating mass M_G at $R = 14 \text{ Mpc}$; as a result, the matter mass $M_M \simeq 2M_G \simeq 2|M_{DE}|$, within this radius. This implies that the antigravity effects are strong indeed at large radii of the Coma cluster.

4. Matter mass profile

Our estimate of the Coma matter mass within $R = 14 \text{ Mpc}$ (Eq.11) may be compared with estimates following from traditional matter density profiles for dark halos. The widely used NFW profile (Navarro et al. 1999) is

$$\rho = \frac{4\rho_s}{\frac{R}{R_s}(1 + \frac{R}{R_s})^2}, \quad (10)$$

where R is again the distance from the cluster center, $\rho_s = \rho(R_s)$, and R_s are constant parameters. At small radii, $R \ll R_s$, the matter density goes to infinity, $\rho \propto 1/R$ as R goes to zero. At long distances, $R \gg R_s$, the density slope is $\rho \propto 1/R^3$. With this profile, the matter mass profile is

$$M_M(R) = 16\pi\rho_s R_s^3 \left[\ln(1 + R/R_s) - \frac{R/R_s}{1 + R/R_s}\right]. \quad (11)$$

To find the parameters ρ_s and R_s , we may use the small-radii data from Sec.1: $M_1 = 4.4 \times 10^{14} M_\odot$ at $R_1 = 1.4 \text{ Mpc}$, $M_2 = 2.6 \times 10^{15} M_\odot$ at $R_2 = 4.8 \text{ Mpc}$. At these radii, the gravitating masses are nearly equal to the matter masses there. The values of M_1, R_1 and M_2, R_2 , together with Eq.11 lead to two logarithmic equations for the two parameters of the profile, which can easily be solved: $R_s = 4.7 \text{ Mpc}$, $\rho_s = 1.8 \times 10^{-28} \text{ g/cm}^3$. Then we find the matter mass within $R = 14 \text{ Mpc}$,

$$M_M \simeq 8.7 \times 10^{15} M_\odot, \quad (12)$$

to be considerably larger (over 70%) than given by Eq.11.

Another popular ρ density profile (Hernquist 1990) is

$$\rho(R) \propto \frac{1}{R(R + \alpha)^3}. \quad (13)$$

Its small-radius behavior is the same as in the NFW profile: $\rho \rightarrow \infty$, as R goes to zero. The slope at large

radii is different: $\rho \propto 1/R^4$. The corresponding mass profile is

$$M_M(R) = M_0 \left[\frac{R}{R + \alpha} \right]^2. \quad (14)$$

The parameters M_0 and α can be found from the same data as above on M_1, R_1 and M_2, R_2 : $M_0 = 1.4 \times 10^{16} M_\odot$, $\alpha = 6.4$ Mpc, giving another value for the mass within 14 Mpc:

$$M_M = 6.6 \times 10^{15} M_\odot, \quad R = 14 \text{ Mpc}. \quad (15)$$

Now the difference from the figure of Eq.9 is about 40%.

In a search for a more suitable mass profile for the Coma cluster, we may try the following simple new relation:

$$M_M(R) = M_* \left[\frac{R}{R + R_*} \right]^3. \quad (16)$$

This mass profile comes from the density profile:

$$\rho(R) = \frac{3}{4\pi} M_* R_* (R + R_*)^{-4}. \quad (17)$$

The density goes to a constant as R goes to zero; at large radii, $\rho \propto 1/R^4$, as in Hernquist's profile.

The parameters M_* and R_* are found again from the data for the radii of 1.4 and 4.8 Mpc: $M_* = 8.7 \times 10^{15} M_\odot$, $R_* = 2.4$ Mpc. The new profile leads to a lower matter mass at 14 Mpc:

$$M_M = 5.4 \times 10^{15} M_\odot, \quad (18)$$

which is equal to the Eq.9 value within 15% accuracy.

5. Upper limits and beyond

The strong effect of dark energy at large radii puts an absolute upper limit on the total size of the cluster. The system can be gravitationally bound only if gravity dominates in its volume (as we mentioned above). In terms of the three different masses, this criterion may be given in the form

$$M_G \geq 0, \quad M_M \geq |M_{DE}|. \quad (19)$$

Both inequalities are met, if the system is not larger than its zero-gravity radius (Eq.5): $R \leq R_{\max} = R_{ZG}$.

If the radius of a system with matter mass M_M is equal to the maximal radius $R = R_{\max}$, its mean matter density (see Bisnovatyi-Kogan & Chernin 2012) is

$$\langle \rho_M \rangle = \frac{M_M}{\frac{4\pi}{3} R_{ZG}^3} = 2\rho_{DE}. \quad (20)$$

This relation and the new profile (Eq.16) now lead to R_{\max} and the corresponding matter mass, $M_{\max} = M_M(R_{\max})$:

$$\begin{aligned} R_{\max} &= R_{ZG} = 20 \text{ Mpc}, \\ M_{\max} &= M_M(R_{ZG}) = 6.2 \times 10^{15} M_\odot. \end{aligned} \quad (21)$$

The upper mass limit evaluated by Eq.(21) is consistent with the theory of large-scale structure formation that claims the range $2 \times 10^{15} < M < 10^{16} M_\odot$ for the most massive bound objects in the Universe (Holz & Perlmutter 2012, Busha et al. 2005)

For comparison, the two profiles mentioned above lead to somewhat larger values of the sizes and mass:

$$R_{\max} = 25 \text{ Mpc}, \quad M_{\max} = 1.5 \times 10^{16} M_\odot \text{ (NFW)}, \quad (22)$$

$$R_{\max} = 22 \text{ Mpc}, \quad M_{\max} = 9.1 \times 10^{15} M_\odot \text{ (Hernquist)}. \quad (23)$$

Our studies of nearby systems like the Local Group and the Virgo and Fornax clusters (Karachentsev et al. 2003, Chernin 2008, Chernin et al. 2006, 2007, 2010, 2012a,b, Chernin 2013) show that their sizes are near the zero-gravity radii. The systems are located in the gravity-dominated regions ($R < R_{ZG}$), and the outflows of galaxies are observed at $R > R_{ZG}$. Basing on these examples, we may suggest that the Coma cluster has the maximal possible size and mass given by Eq.(21). If this is the case, the mean matter density of the system = twice the dark energy density. This prediction (Merafina et al. 2012; Bisnovatyi-Kogan & Chernin 2012) does not depend on the density profile assumed for the cluster. Basing on this result and using the cosmological matter density parameter $\Omega_m = 0.27$, we may calculate the mean matter density contrast in the cluster:

$$\delta = \frac{\langle \rho \rangle - \rho_m}{\rho_m} = \frac{2\Omega_{DE}}{\Omega_m} - 1 = 4.2. \quad (24)$$

An observational confirmation of this figure would directly indicate the key role of dark energy in the formation of the structure of the system.

Another general prediction based on the same analogy with the earlier studied groups and clusters concerns the galaxies in the environment of the Coma cluster. We may assume that beyond the Coma size limit, at $R > R_{\max} = R_{ZG}$, there are galaxies that are not gravitationally bound with the cluster and move away from it. They may form a quasi-regular outflow in the area of the dark energy domination. The radial motions of the outflow galaxies are controlled by the equation of motion that takes into account both gravity and antigravity forces given by Eqs.(4):

$$\ddot{R} = -G \frac{M_M}{R^2} + \frac{8\pi G}{3} \rho_{DE} R, \quad (25)$$

where M_M is the total matter mass of the cluster and $R \geq R_{ZG}$.

The first integral of the equation of motion is the mechanical energy of a galaxy (per unit mass):

$$E = \frac{1}{2} V^2 - \frac{GM_M}{R} - \frac{4\pi G}{3} \rho_{DE} R^2. \quad (26)$$

It is seen from Eq.(25) that at large distances, at $R \gg R_{\max} = R_{ZG}$, the flow tends to the regular

kinematical structure with the Hubble linear velocity-distance relation:

$$V(R) \rightarrow H_{\Lambda} R, \quad (27)$$

where $H_{\Lambda} = [\frac{8\pi G}{3}\rho_{\text{DE}}]^{1/2} = 61 \text{ km/s/Mpc}$ depends on the dark energy density only.

It is also seen from Eq.(26) that at all distances $R \geq R_{\text{max}} = R_{\text{ZG}}$ the outflow velocities are higher than a critical value:

$$V \geq V_{\text{esc}} = H_{\Lambda} R [1 + 2(R_{\text{ZG}}/R)^3 - 3(R_{\text{ZG}}/R)^2]^{1/2}. \quad (28)$$

The value V_{esc} corresponds to the minimal mechanical energy

$$E_{\text{esc}} = -\frac{3}{2} H_{\Lambda}^2 R_{\text{ZG}}^2, \quad (29)$$

needed for a particle to leave the potential well of the cluster and join the outflow. The lower limit for the outflow velocities is the theory prediction which may be tested in current and future observations of the Coma environment.

6. Newtonian approximation in description of galactic winds in presence of DE

In the Newtonian approximation, in presence of DE, we have the following hydrodynamic Euler equation for the spherically symmetric outflow in the gravitational field of matter and DE

$$\begin{aligned} \rho v \frac{dv}{dr} + \frac{dP}{dr} &= -\rho \left(\frac{Gm_m}{r^2} - \frac{\Lambda c^2 r}{3} \right) \quad (30) \\ &= -\rho \left(\frac{Gm_m}{r^2} - \frac{8\pi G \rho_{\Lambda} r}{3} \right). \end{aligned}$$

Here ρ and P are a matter density and pressure, respectively, m_m is the mass of the matter inside the radius r . We use here DE in the form of the Einstein cosmological constant Λ . Newtonian gravitational potentials produced by matter Φ_g , and Φ_{Λ} by DE, satisfy the Poisson equations

$$\Delta \Phi_{\Lambda} = -8\pi G \rho_{\Lambda}, \quad \Delta \Phi_g = 4\pi G \rho, \quad \rho_{\Lambda} = \frac{\Lambda c^2}{8\pi G}. \quad (31)$$

We consider, for simplicity, the outflow in the field of a constant mass (like in stellar wind) $m_m = M$. The Eq. (30) in this case is written as

$$\begin{aligned} \rho v \frac{dv}{dr} + \frac{dP}{dr} &= -\rho \left(\frac{GM}{r^2} - \frac{\Lambda c^2 r}{3} \right) \quad (32) \\ &= -\rho \left(\frac{GM}{r^2} - \frac{8\pi G \rho_{\Lambda} r}{3} \right). \end{aligned}$$

The Eq. (30) should be solved together with the continuity equation in the form

$$4\pi \rho v r^2 = \dot{M}, \quad (33)$$

where \dot{M} is the constant mass flux from the cluster. We consider polytropic equation of state, where pressure P , and sound speed c_s are defined as

$$\begin{aligned} P &= K \rho^{\gamma}, \quad c_s^2 = \gamma \frac{P}{\rho}, \quad \rho = \left(\frac{c_s^2}{\gamma K} \right)^{\frac{1}{\gamma-1}}, \quad (34) \\ P &= \left(\frac{c_s^2}{\gamma} \right)^{\frac{\gamma}{\gamma-1}} K^{-\frac{1}{\gamma-1}}. \end{aligned}$$

Introduce nondimensional variables as

$$\begin{aligned} \tilde{v} &= \frac{v}{v_*}, \quad \tilde{c}_s = \frac{c_s}{c_*}, \quad \tilde{r} = \frac{r}{r_*}, \quad r_* = \frac{GM}{c_*^2}, \quad v_* = c_*, \\ \tilde{\rho} &= \frac{\rho}{\rho_*}, \quad \tilde{P} = \frac{P}{P_*}, \quad \rho_* = \left(\frac{c_*^2}{\gamma K} \right)^{\frac{1}{\gamma-1}}, \quad (35) \\ P_* &= \left(\frac{c_*^2}{\gamma} \right)^{\frac{\gamma}{\gamma-1}} K^{-\frac{1}{\gamma-1}}. \end{aligned}$$

In non-dimensional variables the equation (32) is written as

$$\tilde{v} \frac{d\tilde{v}}{d\tilde{r}} + \frac{2}{\gamma-1} \tilde{c}_s \frac{d\tilde{c}_s}{d\tilde{r}} + \frac{1}{\tilde{r}^2} - \lambda \tilde{r} = 0, \quad \lambda = \frac{\Lambda c_*^2 r_*^2}{3c_*^2}. \quad (36)$$

The continuity equation (33) in non-dimensional form is written as

$$\tilde{\rho} \tilde{v} \tilde{r}^2 = \dot{m}, \quad \tilde{c}_s^{\frac{2}{\gamma-1}} \tilde{v} \tilde{r}^2 = \dot{m}, \quad \dot{m} = \frac{\dot{M}}{M_*}, \quad (37)$$

$$\dot{M}_* = 4\pi \rho_* v_* r_*^2.$$

It follows from (34),(35),(37), that

$$\frac{d\tilde{\rho}}{\tilde{\rho}} = \frac{2}{\gamma-1} \frac{d\tilde{c}_s}{\tilde{c}_s}, \quad \frac{d\tilde{\rho}}{\tilde{\rho}} + \frac{d\tilde{v}}{\tilde{v}} + 2 \frac{d\tilde{r}}{\tilde{r}} = 0. \quad (38)$$

Using (38) we may write the equation of motion (36) in the form

$$\frac{d\tilde{v}}{d\tilde{r}} = \frac{\tilde{v}}{\tilde{r}} \frac{2\tilde{c}_s^2 - \frac{1}{\tilde{r}} + \lambda \tilde{r}^2}{\tilde{v}^2 - \tilde{c}_s^2}. \quad (39)$$

The only physically relevant solutions are those which pass smoothly the sonic point $v = c_s$, being a singular point of the Eq. (10), with

$$\tilde{v} = \tilde{c}_s, \quad 2\tilde{c}_s^2 - \frac{1}{\tilde{r}} + \lambda \tilde{r}^2 = 0 \quad (40)$$

where $\tilde{r} = \tilde{r}_c$, $\tilde{v} = \tilde{v}_c$, $\tilde{c}_s = \tilde{c}_{sc}$. Choosing $c_* = c_{sc}$, we obtain in the critical point

$$\tilde{v}_c = \tilde{c}_{sc} = 1, \quad 2 - \frac{1}{\tilde{r}_c} + \lambda \tilde{r}_c^2 = 0. \quad (41)$$

With this choice of the scaling parameters, we have from (37)

$$\dot{m} = \tilde{r}_c^2. \quad (42)$$

The physical meaning of the parameter λ becomes clear after rewriting it, using (31),(35), in the form

$$\lambda = \frac{\Lambda c^2 r_*^2}{3c_s^2} = \rho_\Lambda \frac{8\pi}{3M} r_*^3 = \rho_\Lambda \frac{8\pi}{3M} \frac{r_c^3}{\tilde{r}_c^3} = \frac{2\rho_\Lambda}{\rho_M} \frac{1}{\tilde{r}_c^3}, \quad (43)$$

where $\rho_M = \frac{3M}{4\pi r_c^3}$ is a density of the matter after smearing the central mass uniformly inside the critical radius r_c . The value of λ is proportional to the ratio of the dark energy mass inside the critical radius $M_\Lambda = \frac{4\pi}{3} r_c^3 \rho_\Lambda$ to the mass M of the central body.

The relation (41) determines the dependence $\tilde{r}_c(\lambda)$ in the solution for the galactic wind and accretion, in presence of DE. In presence of DE the critical radius of the flow is situated closer to the gravitating center (in non-dimensional units) with increasing λ . The Eq.(36) for the polytropic flow has a Bernoulli integral as

$$\frac{\tilde{v}^2}{2} + \frac{\tilde{c}_s^2}{\gamma-1} - \frac{1}{\tilde{r}} - \frac{\lambda \tilde{r}^2}{2} = h, \quad (44)$$

$$\tilde{c}_s^2 = \left(\frac{\dot{m}}{\tilde{v} \tilde{r}^2} \right)^{\gamma-1} = \left(\frac{\tilde{r}_c^2}{\tilde{v} \tilde{r}^2} \right)^{\gamma-1}.$$

The dimensional Bernoulli integral $H = hc_{sc}^2$. The Bernoulli integral is determined through the parameters of the critical point, with account of (41), as

$$h = \frac{\gamma+1}{2(\gamma-1)} - \frac{1}{\tilde{r}_c} - \frac{\lambda \tilde{r}_c^2}{2} = \frac{5-3\gamma}{2(\gamma-1)} - \frac{3}{2} \left(\frac{1}{\tilde{r}_c} - 2 \right). \quad (45)$$

The dependence $h(\lambda)$ for different polytropic powers γ is given in Fig.1. Note that in presence of DE the outflow is possible also for negative values of the Bernoulli integral h , defined equally.

The stationary solution for the wind is determined by two integrals: constant mass flux \dot{M} , and energy (Bernoulli) integral H . In absence of DE we obtain the known relations

$$\tilde{r}_c = \frac{1}{2}, \quad h = \frac{5-3\gamma}{2(\gamma-1)}. \quad (46)$$

At small λ we have from (41),(45)

$$\tilde{r}_c = 0.5 - \frac{\lambda}{16}, \quad h = \frac{5-3\gamma}{2(\gamma-1)} - \frac{3}{8}\lambda \quad (47)$$

At large $\lambda \rightarrow \infty$ it follows from (41) $\tilde{r}_c \rightarrow \tilde{r}_{c\infty} = \lambda^{-1/3}$. Making expansion in (41) around $\tilde{r}_{c\infty}$ in the form

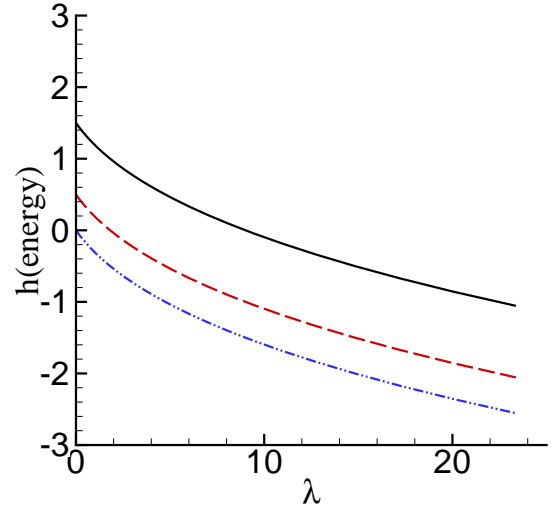


Figure 1: The function $h(\lambda)$ for $\gamma = \frac{4}{3}$ (full curve); $\gamma = \frac{3}{2}$ (dashed curve); $\gamma = \frac{5}{3}$ (dash-dot-dot curve), according to relations (41),(45)

$$\frac{1}{\tilde{r}_c} = \lambda^{1/3} + \varepsilon,$$

we obtain from (41), (45)

$$\begin{aligned} \varepsilon &= \frac{2}{3}, \quad \tilde{r}_c = \frac{1}{\lambda^{1/3} + \frac{2}{3}}, \quad h = \frac{5-3\gamma}{2(\gamma-1)} - \frac{3}{2}\lambda^{1/3} + 2 \\ &= \frac{\gamma+1}{2(\gamma-1)} - \frac{3}{2}\lambda^{1/3} \quad \text{at } \lambda \rightarrow \infty. \end{aligned} \quad (48)$$

In the outflow from the physically relevant quasi-stationary object the antigravity from DE should be less than the gravitational force on the outer boundary, which we define at $r = r_*$. Therefore the value of Λ is restricted by the relation (see e.g. Bisnovatyi-Kogan and Chernin, 2012)

$$2\rho_\Lambda = \frac{\Lambda c^2}{4\pi G} < \bar{\rho} = \frac{4\pi M}{3r_*^3} \quad (49)$$

In non-dimensional variables this restriction, with account of (35),(36) is written as

$$\lambda < \frac{16\pi^2}{9} = 17.55 = \lambda_{lim}. \quad (50)$$

It is reasonable to consider only the values of λ smaller than λ_{lim} . It follows from (41), that \tilde{r}_c is monotonically decreasing with increasing λ . For $\lambda = \lambda_{lim} = 17.55$ we obtain $\tilde{r}_c = \tilde{r}_{c,lim} \approx 0.29$. The effective gravitational potential $\tilde{\Phi}$ is formed by the gravity of the central body, and antigravity of DE

$$\tilde{\Phi} = -\frac{1}{\tilde{r}} - \frac{\lambda \tilde{r}^2}{2}. \quad (51)$$

To overcome the gravity of the central body, the value of h should exceed the maximum value of the gravitational potential, defined by the extremum of $\tilde{\Phi}$

$$h \geq \tilde{\Phi}_{max}(\tilde{r}_{max}) = -\frac{3}{2}\lambda^{1/3}, \quad \tilde{r}_{max} = \lambda^{-1/3}. \quad (52)$$

It follows from(41), (52), that always $\tilde{r}_{max} > \tilde{r}_c$. So, in presence of DE the outflow of the gas from the cluster to the infinity is possible even at the negative values of h . In absence of DE the non-negative value of h , and the outflow are possible only at $\gamma \leq \frac{5}{3}$.

7. Solutions of the galactic wind equation in presence of DE

The equation (39) has a sound critical point of the saddle type, and two physical (critical) solutions going through this critical point. One of this solutions describes a wind outflow, and has a positive \tilde{v} . Another solution corresponds to an accretion (inflow), and has a negative \tilde{v} (Stanyukovich, 1955; Parker, 1963). To obtain a physically relevant critical solution of (39), with \tilde{c}_s^2 from (44), we obtain expansion in the critical point with $\tilde{v}^2 = \tilde{c}_s^2 = 1$, in the form

$$\begin{aligned} \tilde{v} &= 1 + \alpha(\tilde{r} - \tilde{r}_c), \quad \alpha_1 = -\frac{2}{\tilde{r}_c} \frac{\gamma - 1}{\gamma + 1}, \\ &+ \frac{1}{\tilde{r}_c} \frac{2}{\gamma + 1} \sqrt{2 + \frac{1}{4\tilde{r}_c} + \frac{\lambda\tilde{r}_c^2}{2} - \gamma \left(2 - \frac{1}{4\tilde{r}_c} - \frac{\lambda\tilde{r}_c^2}{2}\right)}, \\ \alpha_2 &= -\frac{2}{\tilde{r}_c} \frac{\gamma - 1}{\gamma + 1} \quad (53) \\ &- \frac{1}{\tilde{r}_c} \frac{2}{\gamma + 1} \sqrt{2 + \frac{1}{4\tilde{r}_c} + \frac{\lambda\tilde{r}_c^2}{2} - \gamma \left(2 - \frac{1}{4\tilde{r}_c} - \frac{\lambda\tilde{r}_c^2}{2}\right)}. \end{aligned}$$

Here α_1 corresponds to the wind solution, and α_2 is related to the case of accretion where \tilde{v} define the absolute value. At $\lambda = 0$ we have a well known expansion with

$$\begin{aligned} \alpha_1 &= \frac{4}{\gamma + 1} \left[\sqrt{\frac{5 - 3\gamma}{2}} - (\gamma - 1) \right], \\ \alpha_2 &= -\frac{4}{\gamma + 1} \left[\sqrt{\frac{5 - 3\gamma}{2}} + (\gamma - 1) \right]. \end{aligned}$$

It follows from the expansion (53), that physically relevant solutions exist only with positive value under the square root. It give the restriction for the value of γ as a function of λ in the form

$$\gamma \leq \gamma_{max} = \frac{2 + \frac{1}{4\tilde{r}_c} + \frac{\lambda\tilde{r}_c^2}{2}}{2 - \frac{1}{4\tilde{r}_c} - \frac{\lambda\tilde{r}_c^2}{2}}.$$

At $\lambda = 32$, $\tilde{r}_c = 0.25$ the limiting value γ_{max} goes to ∞ , so that at $\lambda \geq 32$ the wind solutions exist formally for all polytropic powers γ .

The numerical solution of (39) was obtained using predictor-corrector Runge-Kutta method of 4-th order, with a fixed relative precision, written in Fortran 77, see Press et al. (1992) The integration started from the critical point with $\tilde{v} = \tilde{c}_s = 1$, using the expansion (53), both inside and outside the critical point, for two types of the flow: the wind flow, corresponding to the coefficient α_1 in (53), and accretion flow, corresponding to α_2 in (53). The critical solutions of the equation (39), with account of (44), are presented in Figs.2,3 for different values of γ and λ . Both wind and accretion solutions are presented.

The wind and accretion solutions are plotted in the same figures 2,3, but the positive velocities correspond only to the wind solutions. The outflow solutions have increasing velocities in presence of DE with $\lambda > 1$, but at $\lambda = 0$ the behaviour at large radius \tilde{r} depends on the adiabatic power γ . The velocity is increasing in the wind solution at $\gamma = \frac{4}{3}$ (Fig.2). At $\gamma = \frac{5}{3}$ the wind solution has a decreasing outflow velocity with a constant Mach number, see Fig.3.

The accretion solutions in Figs.2,3 are represented by the absolute values of the inflow velocity $|\tilde{v}|$, and the inflow velocity during accretion has a negative sign. The inflow velocity inside the critical point at $\gamma = \frac{4}{3}$ at all λ converges to the same free fall velocity $\tilde{v} \rightarrow -\sqrt{\frac{2}{\tilde{r}}}$, according to the Bernoulli integral (44), with $\tilde{r} \ll 1$, in the supersonic flow with $\tilde{v} \gg \tilde{c}_s$. At $\gamma = \frac{5}{3}$ the inflow solution at $\tilde{r} \ll 1$ is approaching to the constant Mach number solution. The inflow solutions given in Fig.3 correspond to $Ma = 1$. The equation (39) is invariant to the transformation $\tilde{v} \rightarrow -\tilde{v}$, therefore the accretion solution was possible to obtain numerically for the absolute values of the velocity.

The inflow solutions for the accretion starts at large radiuses by a slow motion to the gravitating center. The velocity increases in a subsonic regime, and after crossing the critical point the supersonic infall to the gravitating center starts. Note, that the accretion solutions have a physical sense only for small λ , when the region with a attractive gravitational force is sufficiently large. In the regions with repulsing force due to DE antigravity, the critical accretion solutions of the equation (39) formally exist, but they correspond to anomalous density distribution increasing with radius, what cannot be expected in reality.

8. Discussion

It is clear that the presence of DE tends to help the outflow of the hot gas from the gravitating ob-

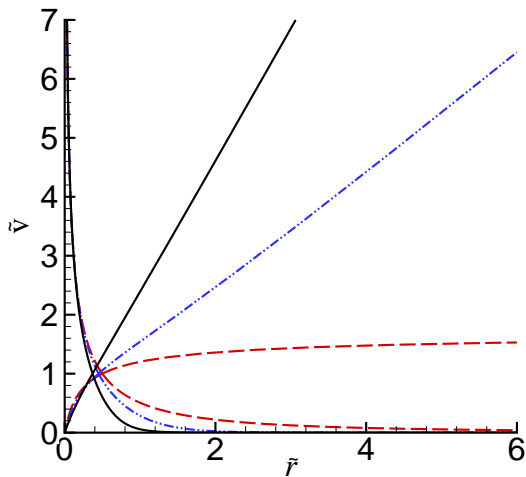


Figure 2: The integral curves of the equations (39), (44), for $\gamma = 4/3$ and $\lambda = 0$, $r_c=0.5$ (dashed curves); $\lambda = 1.10$, $r_c = 0.45$ (dash-dot-dot curves); and $\lambda = 5.13$, $r_c = 0.37$ (full curves). Wind solutions correspond to curves with increasing velocity at large radius. The curves with decreasing velocities correspond to the accretion solution with negative v , so that its absolute value is presented.

ject, as well as to the escape of rapidly moving galaxies (Chernin et al, 2013). Here we have obtained the solution for outflow in presence of DE, which generalize the well-known solution for the polytropic solar (stellar) wind. Presently the DE density exceed the density of the dark matter, and, even more, the density of the barionic matter. The clusters which outer radius is approaching the zero gravity radius, may not only loose galaxies, which join the process of Hubble expansion, but also may loose the hot gas from the outer parts of the cluster. Let us consider outer parts of the Coma cluster at radius $R_C = 15$ Mpc, with the mass inside $M_C = 5 \cdot 10^{15} M_\odot$, from Chernin et al. (2013). For the present value of $\rho_\Lambda = 0.71 \cdot 10^{-29}$ g/cm³, supposing that $R_C = r_*$ is the critical radius of the wind, we obtain from (2),(7), the nondimensional constant λ as

$$\lambda = \frac{\Lambda c^2 r_*^2}{3c_*^2} = \frac{8\pi \rho_\Lambda r_*^3}{3M} \approx 0.59, \quad (54)$$

$$c_* = \sqrt{\frac{GM_C}{R_C}} \approx 1200 \text{ km/c.}$$

It corresponds to the temperature about $T \approx 6 \cdot 10^7$ K, $kT \approx 5$ keV. Observations of the hot gas distribution in the Coma cluster (Watanabe et al., 1999) on ASCA satellite have shown a presence of hot region with $kT = 11 - 14$ keV, and more extended cool region with $kT = 5 \pm 1$ keV, what is in good accordance with our choice of parameters.

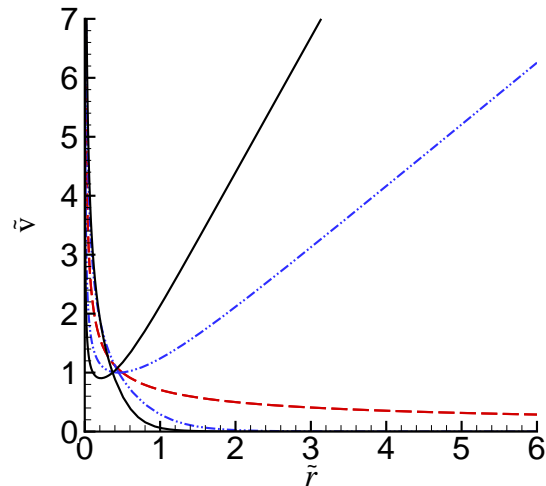


Figure 3: The integral curves of the equations (39), (44), for $\gamma = 5/3$ and $\lambda = 0$, $r_c=0.5$ (dashed curve); $\lambda = 1.10$, $r_c = 0.45$ (dash-dot-dot curves); and $\lambda = 5.13$, $r_c = 0.37$ (full curves). For nonzero λ wind solutions correspond to curves with increasing velocity at large radius. The curves with decreasing velocities correspond to the accretion solution with negative v , so that its absolute values are presented. At $\lambda = 0$ both wind and accretion solutions are presented by the same curve, which corresponds to the wind for positive v , and to the accretion for negative v .

Wind solutions for $\lambda=0$; 0.58; 1.1 are presented in Fig.4. The solution with $\lambda=0.58$ is the closest to the description of the outflow from Coma cluster. The density of the gas in the vicinity of $r = r_c$ is very small, so the flow may be considered as adiabatic (polytropic) with the power $\gamma=5/3$. Without DE such gas flow is inefficient, its velocity is decreasing $\sim 1/\sqrt{r}$, see Eq. (25). In presence of DE the wind velocity is increasing 2 times at the distance of $\sim 5r_c \sim 75$ Mpc from Coma.

After quitting the cluster the gas is moving with acceleration, acting as a snowplough for the intergalactic gas. The shell of matter, forming in such a way, may reach a high velocity, exceeding considerably the speed of galaxies in cluster. If the shell meets another cluster, or another shell moving towards, the collision of such flows may induce a particle acceleration. Due to high speed, large sizes, and low density such collisions may create cosmic rays of the highest possible energy (EHECR). We may expect the largest effect when two clusters move to each other. The influence of DE is decreasing with with a red shift, therefore the acceleration of EHECR in this model should take place in the periphery, or between, the closest rich galaxy clusters.

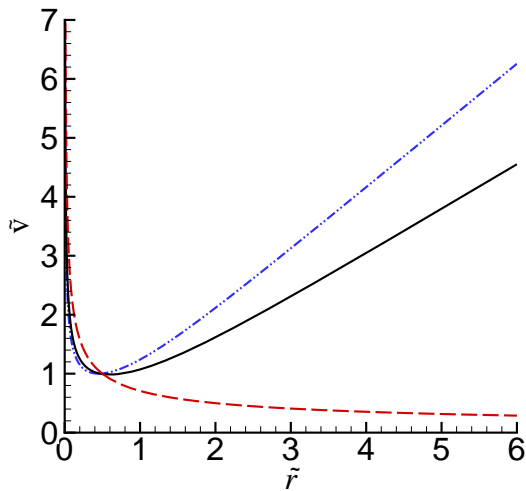


Figure 4: The integral curves of the equations (39), (44) for the wind solution, at $\gamma = 5/3$ and $\lambda = 0$, $r_c=0.5$ (dashed curve); $\lambda = 1.10$, $r_c = 0.45$ (dash-dot dot curve); and $\lambda = 0.58$, $r_c = 0.47$ (full curve).

Acknowledgements. We thank G.G. Byrd, M. Merafina, P. Teerikorpi and M.J. Valtonen for cooperation. Useful discussions with Yu.N. Efremov, I.D. Karachentsev, D.I. Makarov, and A.V. Zasov are appreciated. The work of G.B.-K. was partly supported by RFBR grant 11-02-00602, the RAN Program Formation and evolution of stars and galaxies, and Russian Federation President Grant for Support of Leading Scientific Schools NSH-3458.2010.2.

References

- Bisnovaty-Kogan G.S., Chernin A.D.: 2012, *Ap&SS*, **338**, 337
 Bisnovaty-Kogan G.S., Merafina M.: 2013, *MNRAS*, **434**, 3628
 Busha M.T., Evrard A.E., Adams F.C., Wechsler R.H.: 2005, *MNRAS*, **363**, L11
 Byrd G.G., Chernin A.D., Valtonen M.J.: 2007, *Cosmology: Foundations and Frontiers*, Moscow, URSS
 Byrd G.G., Chernin A.D., Teerikorpi P., Valtonen M.J.: 2012, *Paths to Dark Energy: Theory and Observation*, N.Y., de Gruyter
 Chernin A.D.: 2001, *Physics-Uspekhi*, **44**, 1099
 Chernin A.D.: 2008, *Physics-Uspekhi*, **51**, 267
 Chernin A.D.: 2013, *Physics-Uspekhi*, **56**, 704
 Chernin A.D., Teerikorpi P., Baryshev Yu.V.: 2000, [*astro-ph/0012021*], *Adv. Space Res.*, **31**, 459 (2003)
 Chernin A.D., Teerikorpi P., Baryshev Yu.V.: 2006, *A&A*, **456**, 13
 Chernin A.D., Karachentsev I.D., Kashibadze O.G. et al.: 2007, *Astrophysics*, **50**, 405
 Chernin A.D., Karachentsev I.D., Nasonova O.G. et al.: 2010, *A&A*, **520**, 104
 Chernin A.D., Teerikorpi P., Valtonen M.J. et al.: 2012a, *Astr. Rep.*, **56**, 653
 Chernin A.D., Teerikorpi P., Valtonen M.J. et al.: 2012b, *A&A*, **539**, A4
 Chernin A.D., Bisnovaty-Kogan G.S., Teerikorpi P. et al.: 2013, *A&A*, **553**, 101
 Colles M.: 2006, in *Encyclopedia of Astronomy and Astrophysics*, P.Murdin, ed., IOP Pubs.Ltd, UK, p.245
 Diaferio A.: 1999, *MNRAS*, **309**, 610
 Diaferio A., Geller M.J.: 1997, *ApJ*, **481**, 633
 Geller M.J., Diaferio A., Kurtz M.J.: 1999, *ApJ*, **517**, L23
 Geller M.J., Diaferio A., Kurtz M.J.: 2011, *AJ*, **142**, 143
 Hartwick F.D.A.: 2011, *AJ*, **141**, 198
 Hernquist L.: 1990, *ApJ*, **356**, 359
 Holz D.E., Perlmutter S.: 2012, *ApJL*, **755**, L36
 Hughes J.P.: 1989, *ApJ*, **337**, 21
 Hughes J.P.: 1998, "Untangling Coma Berenices: A New Vision of an Old Cluster", Proceedings of the meeting held in Marseilles, June 17-20, 1997, Eds.: Mazure, A., Casoli F., Durret F., Gerbal D., Word Scientific, p 175.
 Karachentsev I.D., Chernin A.D., Teerikorpi P.: 2003, *Astrophysics*, **46**, 491
 Kubo J.M., Stebbins A., Annis, J. et al.: 2007, *ApJ*, **671**, 1466
 Merafina M., Bisnovaty-Kogan G.S., Tarasov S.O.: 2012, *A&A*, **541**, 84
 Navarro J., Frenk C.S., White S.D.M.: 2005, *ApJ*, **463**, 563
 The L. S., White S.D.M.: 1986, *AJ*, **92**, 1248
 Zwicky F.: 1933, *Helvetica Phys. Acta*, **6**, 110
 Zwicky F.: 1937, *ApJ*, **86**, 217